Lectures in Applied Mathematics
Volume 28, (1991)

Vortex Sheet Computations: Roll-Up, Wakes, Separation

ROBERT KRASNY

Abstract. Chorin's vortex blob method has been proposed as a way to extend vortex sheet motion past the singularity formation time, into the physically important roll-up regime. Basic questions are:

1. Does the vortex blob method converge to an infinite spiral as the smoothing parameter tends to zero?

2. Do vortex blob computations approximate real fluid motion?

This paper will present and discuss three computations which are relevant to these issues: a) periodic roll-up, b) wake patterns in a thin soap film, c) separation at a sharp edge.

1. Introduction. Coherent vortex structures occur in many types of fluid flow such as wakes, jets, and boundary layers. To make progress in the analysis of these flows, one may consider simpler models in which various physical effects are assumed to be small. In the vortex sheet model, a thin shear layer is replaced by a surface across which the tangential component of the fluid velocity has a jump discontinuity. The mathematical study of vortex sheets has advanced in recent years, but many important questions are still open. Vortex sheet motion belongs to the larger field of vortex dynamics, one of the main approaches to understanding fluid turbulence.

Careful numerical experiments have played a key role in advancing the analysis and application of the vortex sheet model. Difficulties arise in computing vortex sheet motion due to short wavelength instability, singularity formation, and spiral roll-up. Chorin's vortex blob method [10,11], in which the vortex sheet's velocity is desingularized, has been proposed to deal with these difficulties. Basic questions concerning this approach are:

1. Does the vortex blob method converge to an infinite spiral as the smoothing parameter tends to zero?

1991 *Mathematics Subject Classification*: 76D05.

A detailed version of this paper will be submitted for publication elsewhere.

Supported in part by GRI Contract #5088-260-1692, NSF Grant DMS-#8801991, ONR URI#N000184-86-K-0684.

2. Do vortex blob computations approximate real fluid motion?

The aim of this paper is to discuss some recent applications of the vortex blob method to vortex sheet motion, and to see how they bear on the foregoing questions. The vortex sheet evolution equation is presented in §2. Numerical evidence demonstrating convergence of the vortex blob approximation, for the case of periodic vortex sheet motion, is reviewed in §3. In §4, vortex blob calculations are compared with experimental wake patterns in a thin soap film due to Couder et al. [14,15]. An extension of the vortex blob method to compute vortex sheet separation at a sharp edge is presented in §5. The method is applied to compute the motion of a thin jet being expelled from a box through a narrow outlet. Finally, §6 summarizes the results.

2. The Vortex Sheet Evolution Equation. A vortex sheet is defined by a curve $z(\Gamma, t)$ in the complex plane, where Γ is the circulation parameter and t is time. The evolution equation is,

$$\overline{\frac{\partial z}{\partial t}}(\Gamma, t) = \int K(z(\Gamma, t) - z(\tilde{\Gamma}, t))d\tilde{\Gamma} \quad , \quad K(z) = \frac{1}{2\pi i z} \, . \tag{2.1}$$

The Cauchy principal value of the integral is taken. The limits of integration and the initial shape $z(\Gamma, 0)$ depend upon the problem considered. The normal component of the induced velocity field is continuous across the sheet, but the tangential component has a jump. Equation (2.1) says that a point on the vortex sheet moves with the average of the two limiting velocities, defined by approaching the curve on either side. This is a special case of the Biot-Savart law, which expresses the velocity as an integral over the vorticity in incompressible flow [2]. This formulation of the initial value problem for vortex sheet motion is due to Birkhoff [5] and Rott [28].

A flat vortex sheet of constant strength, defined by $z(\Gamma, t) = \Gamma$, is an equilibrium solution of (2.1). Linearized stability analysis of this solution shows that short wavelength perturbations can grow arbitrarily fast, a phenomenon known as "Kelvin-Helmholtz instability" in the fluid dynamics literature. Mathematically speaking, this implies that the initial value problem is ill-posed in the sense of Hadamard. However, Sulem et al. [31] have proven that if the initial perturbation is an analytic function of Γ, then the sheet $z(\Gamma, t)$ remains analytic for a positive time interval.

Moore [25] performed a formal asymptotic analysis for small perturbation amplitude ϵ. The results indicate that the vortex sheet loses analyticity at a finite critical time $t_c(\epsilon)$, due to the formation of a branch point in $z(\Gamma, t_c)$, as a function of Γ. Computational studies [23,18,30] support Moore's conclusion and rigorous validity of his approximation for $t < t_c$ has been proven [8].

3. Vortex Sheet Roll-Up. Pullin conjectured that for $t > t_c$, the vortex sheet rolls up into a spiral that grows larger with increasing time [private communication, 1983]. By analogy with self-similar vortex sheet roll-up [27], the spiral should vanish in size as $t \to t_c^+$, but for any $t > t_c$, it should have an infinite number of turns.

Chorin's vortex blob method has been applied to test this idea [10,11,19]. In this method, the singular kernel in (2.1) is replaced by a smoothed

approximation K_δ, such that $K_\delta(z) \to K(z)$ as $\delta \to 0$. For example, in free space one can use,

$$K_\delta(z) = K(z)\frac{|z|^2}{|z|^2+\delta^2}\ . \tag{3.1}$$

Using this kernel in the evolution equation yields a smoothed approximation to the exact vortex sheet. The curve is discretized into a finite number of "vortex blobs" $z_j(t)$, and the desingularized integral is approximated by a quadrature rule,

$$\overline{\frac{dz_j}{dt}} = \sum_k K_\delta(z_j - z_k)\Gamma_k\ . \tag{3.2}$$

The ordinary differential equations (3.2) are integrated in time to obtain the motion of the vortex blobs. In this way, solutions of the desingularized vortex sheet equation can be obtained in which the discretization error is negligible. For fixed $\delta > 0$, the solutions can be computed past the vortex sheet's critical time t_c. If the smoothed solutions converge for $t > t_c$ as $\delta \to 0$, then the limit is a candidate extension of the vortex sheet past the critical time.

Figure 3.1* shows the evolution over one period in Γ for $0 \le t \le 1$, using the smoothing parameter value $\delta = 0.03$. The initial perturbation is a growing linear eigenfunction of amplitude $\epsilon = 0.01$, for which the critical time is $t_c \sim 0.375$ [18]. Computations using $\delta = 0$ do not yield smooth curves for $t > t_c$, in contrast to the rolling up spiral shown in Figure 3.1. The roll-up begins on a small scale, slightly before time $t = 0.5$, and the spiral becomes larger and tighter at later times.

Figure 3.2 documents convergence of the desingularized solutions at time $t = 1$, over the interval $0.03 \le \delta \le 0.25$ [19]. In Figure 3.2a, the x-axis intercepts of one spiral branch are plotted as a function of δ. More spiral turns appear as the value of δ is reduced, but each x-intercept lies on a smooth curve having a well-defined limit. Figure 3.2b shows a closeup of the spiral core for $\delta = 0.03$. These data indicate that the desingularized solutions converge uniformly to a spiral as $\delta \to 0$.

The $\delta = 0.03$ solution was computed in single precision arithmetic, using a Fourier filter to control roundoff error [18]. The computation took about 2 minutes of cpu time on a CRAY YMP computer. Calculations using the smaller value $\delta = 0.02$ become inaccurate at time $t = 1$, due to the amplification of spurious roundoff error perturbations. The Fourier filter prevents this from happening at short times, but it is ineffective at time $t = 1$. Higher precision arithmetic, or a new idea, will be needed in order to compute accurately with smaller values of δ at late times.

This work for the periodic problem, as well as similar results for a vortex sheet with elliptic circulation distribution [20], support Pullin's conjecture that the vortex sheet rolls up into a spiral for $t > t_c$. The vortex blob method therefore gives one possible extension for the vortex sheet's motion

*FIGURES APPEAR AT THE END OF THIS PAPER.

past the singularity formation time. An outstanding question is whether or not the limit depends upon the particular way that the vortex sheet equation is desingularized. Alternative approaches using finite thickness [4], the vortex-in-cell method [33], and viscosity [34], are being investigated. Some steps towards analyzing these limits have been taken [9,16], but more work is needed to sort out the issues of convergence and uniqueness, especially past the critical time.

In practice, vortex blob computations are performed using a fixed value of δ and then one wants to know whether the results correspond in some way to real fluid motion. The next section is concerned with this issue.

4. Wake Patterns. At moderate Reynolds number, the wake behind a bluff body in a streaming flow forms a regular Kármán vortex street, consisting of two staggered rows of oppositely-signed vortices. Such vortex streets are observed in "natural" experiments, where no explicit forcing is introduced. Forced wakes, in which the solid body undergoes periodic oscillations at specific amplitude and frequency, are also studied experimentally.

Couder et al. [14,15] have investigated the wake behind a solid cylinder in a thin two dimensional soap film. They found that various different vortex street patterns can form in the cylinder's wake when the forcing parameters are varied. The unforced wake is a classical Kármán vortex street, but the forced wakes are dominated by vortex couples (i.e. counter-rotating vortex pairs), which propagate away from the wake's centerline. The fact that small amplitude forcing can affect the resulting wake patterns in this manner is an important finding.

A computational study of this problem would be very ambitious if it were to include the unsteady separation process on the solid body and the wake's downstream development. Couder and Basdevant [14] performed psuedo-spectral calculations for the two dimensional Euler equation with a super-dissipativity term included. The calculations showed how vortex couples can arise from the destabilization of a Kármán vortex street, in agreement with experimental results. They also studied the structure and collision of vortex couples, finding conditions under which couples form whose vorticity and stream function are linearly related. In the present work, the vortex blob method was applied to compute the development of wake patterns from specific initial perturbations, for a periodic analog of the experiment.

Consider flow past a bluff body with two separation points, each contributing a shear layer to the wake. Each layer contains circulation predominantly of one sign. Previous studies have typically employed either two arrays of point vortices, two vortex sheets, or two layers of constant vorticity to model such wakes [3,6,7,22,26]. However, the experiments of Couder et al. [14,15] suggest that in some instances the wake can be modeled more economically by a single vortex sheet carrying both positive and negative circulation. This might be the case when the two separation points are very close to one another. In effect, the flow sees a single separating shear layer whose circulation density alternates in sign along the layer. With this in mind, the present computations use a single vortex sheet, with sinusoidal circulation density, to represent the wake. This contrasts with the

Kelvin-Helmholtz computations in §3, for which the circulation density was positive all along the vortex sheet.

Experimental Apparatus and Computational Setup. In the experiments of Couder et al. [14,15], a rectangular wire frame was used to support a two-dimensional soap film. The wake was created by towing a solid cylinder through the film. In the experiments reproduced below from [14], the cylinder moved from left to right. The system was forced by causing the cylinder to oscillate in the streamwise direction at a specific frequency.

In the vortex blob computations, the wake is represented by a vortex sheet $(x(a,t), y(a,t))$, which is periodic in the Lagrangian variable a. The circulation density along the curve is a given function $\sigma(a) = d\Gamma/da$. The Table gives the initial vortex sheet shape and circulation density for the three cases presented. One spatial period was computed ($0 \le a \le 1$), but six periods are plotted in the Figures. In each case, the initial shape $(x(a,0), y(a,0))$ and circulation density $\sigma(a)$ was chosen to simulate a particular experimental wake pattern from [14]. These computations used the value $\delta = 0.3$ for the smoothing parameter.

Table. Initial vortex sheet shape $(x(a,0), y(a,0))$ and circulation density $\sigma(a)$ for the computations in §4.

Figure	$x(a,0)$	$y(a,0)$	$\sigma(a)$
4.1	a	$0.2\sin 2\pi a$	$\sin 2\pi a$
4.2	$a + 0.1\sin 2\pi a$	$0.2\sin 2\pi a$	$\sin 2\pi a$
4.3	$a + 0.05\sin 4\pi a$	$0.05\sin 4\pi a$	$\sin 4\pi a\ ,\ 0 \le a \le 0.5$
		$-0.05\sin 4\pi a$	$-\sin 4\pi a\ ,\ 0.5 \le a \le 1$

Comparison of Computation with Experiment. Figure 4.1b shows the Kármán vortex street created by towing the cylinder at uniform speed, with no explicit forcing. The experimental wake consists of an array of counter-rotating vortices which are staggered on either side of the centerline. The circulation density for the computation was taken to be $\sigma(a) = \sin 2\pi a$. The vortices' staggered position was obtained by putting a transverse sinusoidal perturbation into the vortex sheet's initial shape. The computation in Figure 4.1a shows the development of a regular vortex street which resembles the experiment.

In Figure 4.2b, the experimental wake was forced at the natural shedding frequency. This resulted in an array of vortex couples that propagate away from the centerline on one side, at an oblique angle. A similar-looking array of computed vortex couples is displayed in Figure 4.2a. In this case, the initial vortex sheet shape of Figure 4.1a was modified by including a longitudinal perturbation.

The experimental wake in Figure 4.3b was forced at close to the natural shedding frequency. The resulting vortex couples propagate away from the centerline on both sides. For the computation in Figure 4.3a, the circulation density and initial shape were obtained by patching together two scaled copies of the functions from Figure 4.2a. One copy was reflected about

the line $y = 0$ in order to cause half of the vortex couples to propagate below the centerline. The computed vortex structures closely resemble the experimental ones.

Couder et al. also presented results at higher Reynolds number showing the destabilization of these patterns and the formation of a cloud of vortex couples [14,15]. Vortex blob simulations of such results would be a good deal more expensive than the present computations.

Discussion. The initial shapes and circulation densities used in the computations are simple sinusoidal functions, or a patched combination in the case of Figure 4.3a. It should be noted that a small amount of trial and error went into choosing these specific initial perturbations. Furthermore, it is not clear how to make a definite connection between the initial perturbations in the computations and the forcing parameters in the experiment. Even so, it is significant that within a restricted class of initial conditions, the desingularized vortex sheet model yields good qualitative agreement with experiment. Although the smoothing parameter δ does not correspond precisely to a physical mechanism such as viscosity or finite thickness, these results show that vortex blob computations can capture important features of real flows. The desingularized vortex sheet model displays a sensitivity to small perturbations similar to that observed in the experiment.

An interesting detail is that the initial shape in Figure 4.3a has a sharp corner (i.e. a slope discontinuity) at the parameter values $a = 0$ and $a = 0.5$. These singularities lie on a portion of the curve which is being stretched and as a result, the corners are smoothed out at later times. This finding is relevant to analytical studies of singularity formation in vortex sheets [8].

A vortex-dipole sheet model for a wake has previously been proposed [21]. In that work, computational vortex-dipoles were used to represent the oppositely-signed vorticity that originates in boundary layers, upstream from a single separation point. This effect is not included in the present work. The oppositely-signed vorticity here represents two free shear layers that originate at nearby separation points on a bluff body.

A serious deficiency of the present vortex sheet model is the artificial nature of the initial and boundary conditions. An important and difficult challenge is to incorporate the unsteady separation process on the solid body and the spatial growth of the wake. Along these lines, a method for treating vortex sheet separation at a sharp edge has been developed and is described in the next section.

5. Separation at a Sharp Edge. Boundary layer separation affects the pressure distribution and forces felt by a solid surface in the flow. Therefore, applications in aerodynamics and ship hydrodynamics require a modeling capability for unsteady separation. This section begins by discussing the flow around a flat plate which is impulsively set into uniform motion in the direction normal to the plate. The fluid is taken to be ideal, i.e. incompressible, inviscid and irrotational, apart from the presence of embedded vortex sheets.

Background. There are two possible ideal flows which are consistent with the impulsively started normal motion of a flat plate. The first possibility is steady flow in a frame moving with the plate, with a bound vortex sheet on the plate. The fluid velocity is infinite at the edges, no vorticity is shed and the flow has no wake. Experiments show however that thin shear layers are shed at the edges of a moving plate [32]. Therefore, this first example of ideal flow is a poor approximation to the real flow behind an impulsively started plate.

It is important to realize that fluid viscosity, however small, would produce vortex shedding at the plate's edges. This effect is implicitly accounted for in the second example - unsteady ideal flow containing free vortex sheets that emanate from the plate's edges. This flow is a candidate asymptotic outer solution to the corresponding viscous flow problem, in the zero viscosity limit. Such ideas go back to Prandtl, although full justification remains to be accomplished.

Several issues arise in computing vortex sheet separation at a sharp edge:
- satisfying the flow tangency condition on the plate.
- implementing the unsteady Kutta condition at the edges.
- initiating vortex shedding.

Previous numerical studies have used the point vortex method to represent the free vortex sheets, (e.g. [29], see also the review by Graham [17]). Recent computations using the vortex blob method have not obtained smooth spiral roll-up [12,13,24]. The present work seeks to develop an improved vortex blob algorithm for the problem. In particular, one criterion is that the method should converge with respect to refinement in the mesh size and the smoothing parameter.

Numerical Method. The plate coincides with the interval $-1 \leq x \leq 1$ for time $t < 0$, and it moves vertically with speed $1/2$ for time $t > 0$. The flow contains a bound vortex sheet on the plate and free vortex sheets emanating from each edge of the plate. The free vortex sheets are represented by vortex blobs, in order to capture their roll-up into spirals. To accurately satisfy the flow tangency condition on the plate, the bound vortex sheet is represented by point vortices. The free vortex sheets are generated by shedding vortex blobs from the edges at each time step.

Let (x_j, y_j) be the position of a vortex element (either a vortex blob or a point vortex) having strength Γ_j. The induced velocity at one of the elements is given by,

$$(5.1) \qquad (\frac{dx_j}{dt}, \frac{dy_j}{dt}) = \sum_{k \neq j} \frac{(-(y_j - y_k)\ ,\ (x_j - x_k))\Gamma_k}{2\pi\ ((x_j - x_k)^2 + (y_j - y_k)^2 + \delta^2)}\ .$$

The sum in (5.1) is taken with the understanding that δ is set equal to zero when the index k corresponds to one of the bound point vortices.

The bound vortex sheet strength $\sigma(x,t)$ satisfies a Cauchy singular integral equation of the 1st kind along the plate,

$$(5.2) \qquad \frac{1}{2\pi} \int_{-1}^{1} \frac{\sigma(\tilde{x},t)d\tilde{x}}{(x - \tilde{x})} = -\ v(x,t)\ .$$

The right side in (5.2) is the normal velocity on the plate which is induced by the free vortex sheets. The reason for using point vortices on the plate is that equation (5.2) could not be solved for a general right side if the kernel were smoothed. To provide better resolution at the edges, the bound point vortices are placed at $x_j = \cos\theta_j, \theta_j = j\pi/n$, and equation (5.2) is satisfied at the midpoint of each interval. The total amount of bound and free circulation is set to zero in accordance with Kelvin's theorem. The linear system of equations for $\sigma(x_j, t)$ is solved by Gaussian elimination.

The total circulation $\Gamma(t)$ in each free vortex sheet is determined by the unsteady Kutta condition,

$$\frac{d\Gamma}{dt} = \frac{1}{2}\,(U_-^2 - U_+^2) = \overline{U}\cdot\sigma\ , \tag{5.3}$$

where U_- and U_+ are the one-sided velocities at the edge, $\overline{U}$ is the average velocity, and σ is the vortex sheet strength at the edge. The average velocity $\overline{U}$ is induced by the free vortex sheets, and $\sigma \sim \Delta\Gamma/\Delta x$ is calculated by a finite difference formula applied to the bound circulation. The one-sided edge velocities only contribute if they correspond to separating (rather than attached) flow. This is responsible for initiating the vortex shedding at time $t = 0$.

The ordinary differential equations (5.1,5.3) were solved by the fourth order Runge-Kutta method with a variable time step. An adaptive mesh parameter controlled the insertion of new points where required due to curve stretching.

Results. Figure 5.1 was obtained using the smoothing parameter value $\delta = 0.2$. The free vortex sheets roll up smoothly. At short times, the vortices are circular in shape but by time $t = 8$, the outer turns have been deformed due to the strain field of the neighboring vortex. Figure 5.2 is a similar result obtained with the smoothing parameter value $\delta = 0.1$. With a smaller amount of smoothing, the curve rolls up more tightly.

Figure 5.3 shows the computed velocity field at time $t = 8$ in a frame of reference that is moving with the plate. The velocity vectors are plotted on a regular grid with a small square at the base of each vector. The vortex blobs and point vortices representing the free and bound vortex sheets are plotted as a sequence of points. A pair of counter-rotating vortices forms in the recirculating region behind the plate. Two stagnation points occur along the centerline - one at the center of the plate and one at the end of the wake.

Validation. In order to validate the algorithm, a comparison with Pullin's [27] computation of self-similar vortex sheet roll-up past a semi-infinite flat plate has been performed. Pullin formulated the problem in self-similar variables and solved for the vortex sheet shape numerically. This avoids the difficulties and expense associated with solving the initial value problem. Pullin used point vortices to represent the free vortex sheet, a single point vortex to represent the inner spiral turns, and conformal mapping to determine the strength of the bound vortex sheet.

Figure 5.4 shows the vortex blob results obtained over the time interval $0 \le t \le 1$, with smoothing parameter values $0.025 \le \delta \le 0.1$. Figure 5.5 compares the $\delta = 0.025$ calculation at time $t = 1$ with Pullin's result. It

may be checked by superimposing the results that the vortex sheet shapes and positions computed by the two methods agree quite well. Figure 5.6a plots the total amount of circulation shed as a function of time, and Figure 5.6b shows the trajectory of the vortex core. The straight lines plotted describe the self-similar solution. As δ becomes smaller, there is better agreement between the unsteady vortex blob result and the self-similar solution. A more detailed comparison will be presented elsewhere.

Instability of a Jet. In order to demonstrate potential applications of the method, a calculation was set up to compute the motion of a jet being expelled from a box. The jet exits through a narrow outlet on the top of the box. A line of passive markers, initially lying across the outlet, is also tracked in time. The jet is driven by two point sources, in the lower left and right corners of the box, which were turned on at time $t = 0$.

The calculated results are shown in Figure 5.6. A starting vortex forms and propagates away from the outlet, leaving behind a thin straight jet. Eventually, a wave forms along the jet and rolls up into a vortex, which catches up to and propagates through the starting vortex. The same process is being repeated further behind in the last frame. Note that no explicit perturbation is needed to generate the secondary vortices - they apparently result from the thinning of the jet where it meets the starting vortex.

Discussion. The method is capable of simulating vortex sheet roll-up at a sharp edge, although the innermost turns in any particular computation depend upon the value of the smoothing parameter. Further testing to determine the effect of numerical parameters is desireable. Still, the good agreement with Pullin's self-similar solution is encouraging.

The desingularized vortex sheet model for separation at a sharp edge does not explicitly mention fluid viscosity. The effect of viscosity is implicitly accounted for by shedding vorticity via the unsteady Kutta condition. A more familiar separation model consists of the Navier-Stokes equations, with the no-slip boundary condition along solid surfaces. However, the Navier-Stokes model becomes numerically intractable at high Reynolds number, due to increased computational costs. The reason for pursuing the desingularized vortex sheet model is the possibility that it may provide a useful alternative to complement the Navier-Stokes model. Comparison of numerical solutions and laboratory experiment is needed in order to assess this possibility.

6. Summary. Strong numerical evidence indicates that the vortex blob method converges past the vortex sheet singularity formation time, as the smoothing parameter tends to zero. The limit curve is a tight spiral with an infinite number of turns. Rigorous proof of this assertion is an open problem.

Periodic vortex blob computations can capture important dynamical features seen in real wakes. In order to bring the model closer to laboratory experiment, a method for computing vortex sheet roll-up past a sharp edge was presented. Good agreement with Pullin's self-similar solution was obtained. The method is applied to compute the wake behind an impulsively started flat plate and the instability of a thin jet.

Acknowledgements. I thank Professors Yves Couder and Dale Pullin for permission to reproduce figures from their published papers. The computations were performed at the NSF San Diego Supercomputer Center and the University of Michigan.

FIGURES

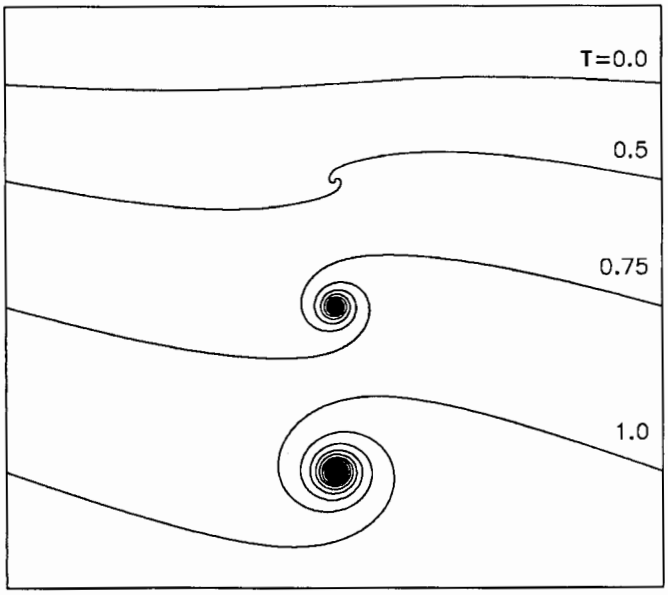

Figure 3.1 Desingularized vortex sheet evolution, computed using the smoothing parameter value $\delta = 0.03$. One period is plotted for times $0 \leq t \leq 1$.

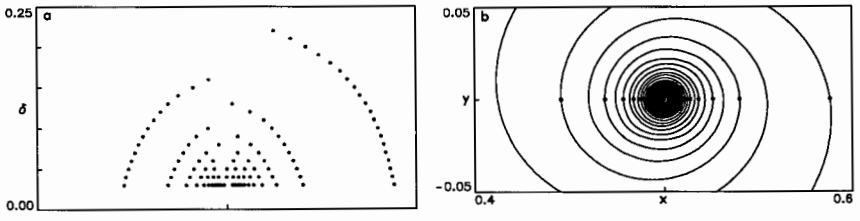

Figure 3.2 Convergence as $\delta \to 0$ at time $t = 1$. a) The x-axis intercepts of one spiral branch are plotted against values of the smoothing parameter in the interval $0.03 \leq \delta \leq 0.25$. b) A closeup view of the spiral obtained using $\delta = 0.03$.

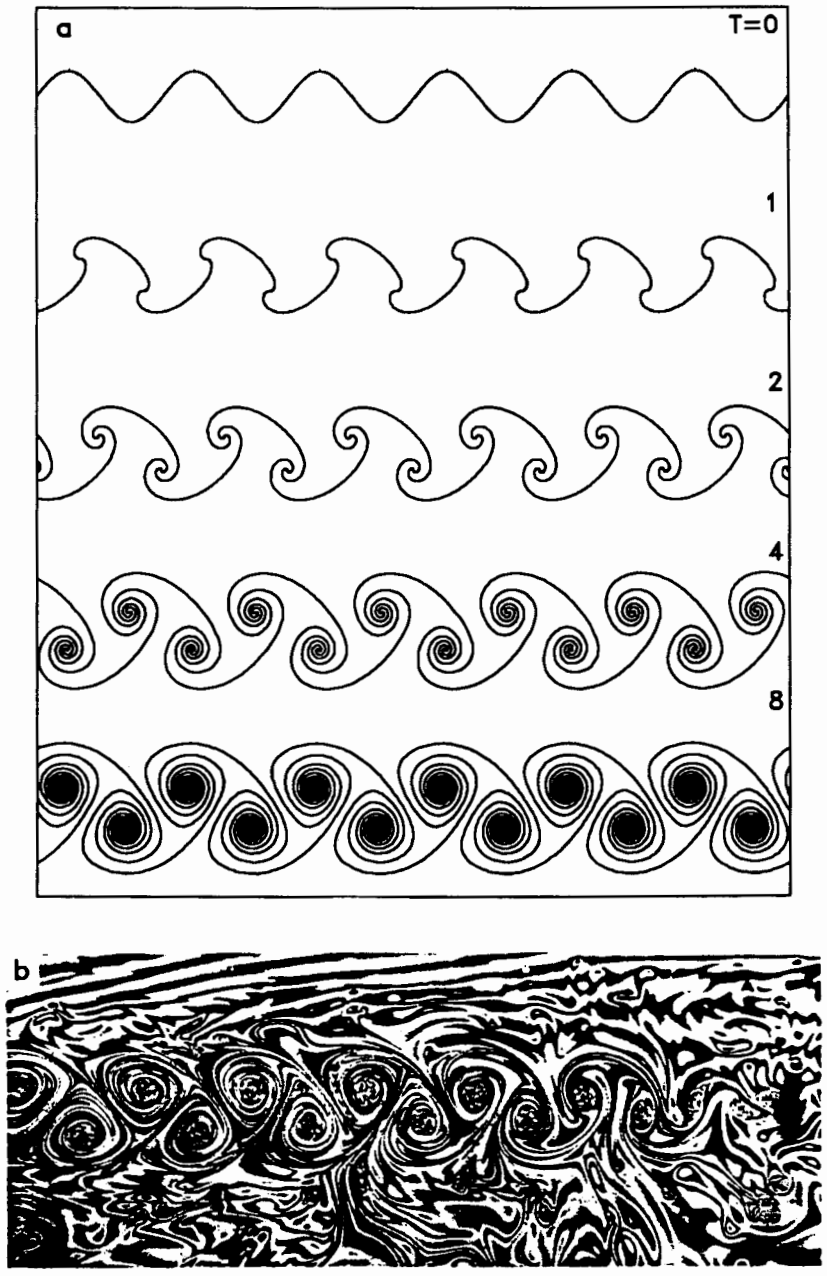

Figure 4.1 a) Vortex blob computation using a transverse sinusoidal perturbation in the initial shape. b) With no explicit forcing, a regular Kármán vortex street forms (experiment reproduced from Couder and Basdevant [14]).

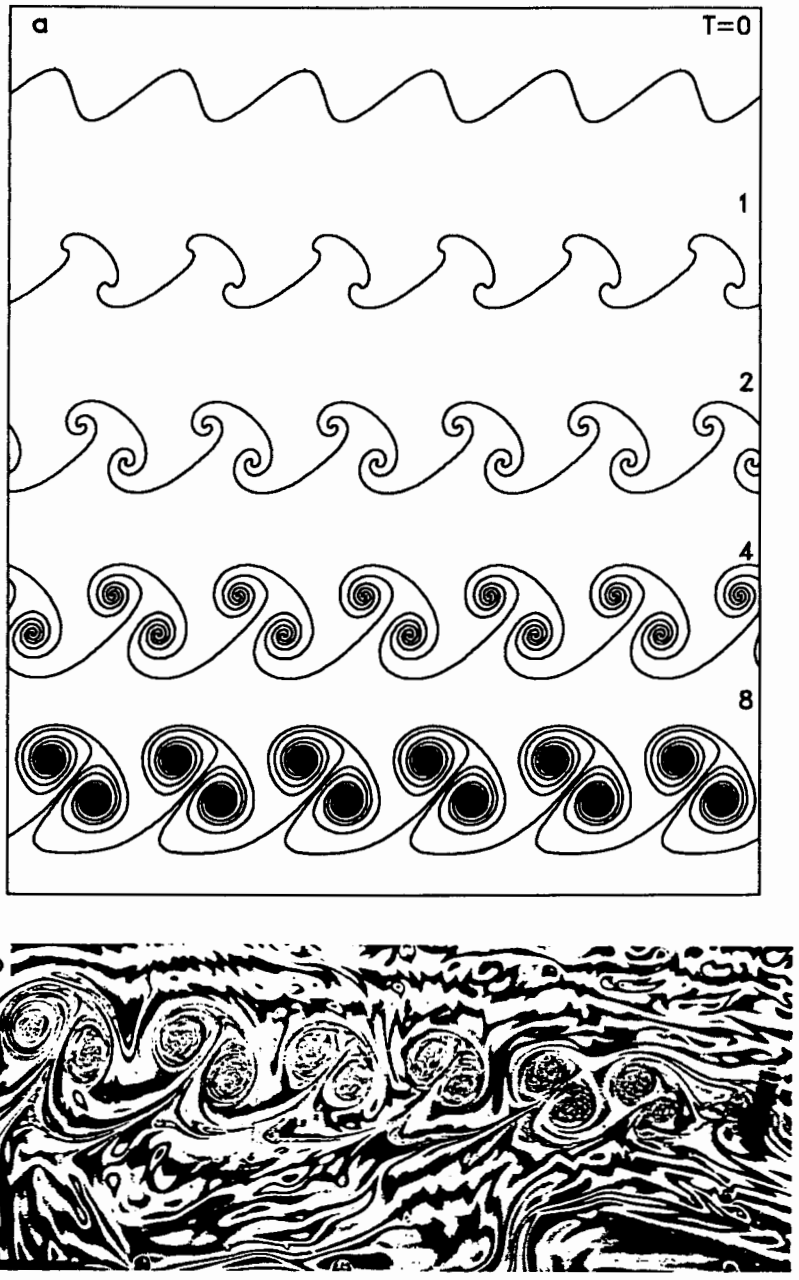

Figure 4.2 a) Computation including transverse and longitudinal perturbations in the initial shape. b) Forcing at the natural shedding frequency produces an array of vortex couples (experiment reproduced from Couder and Basdevant [14).

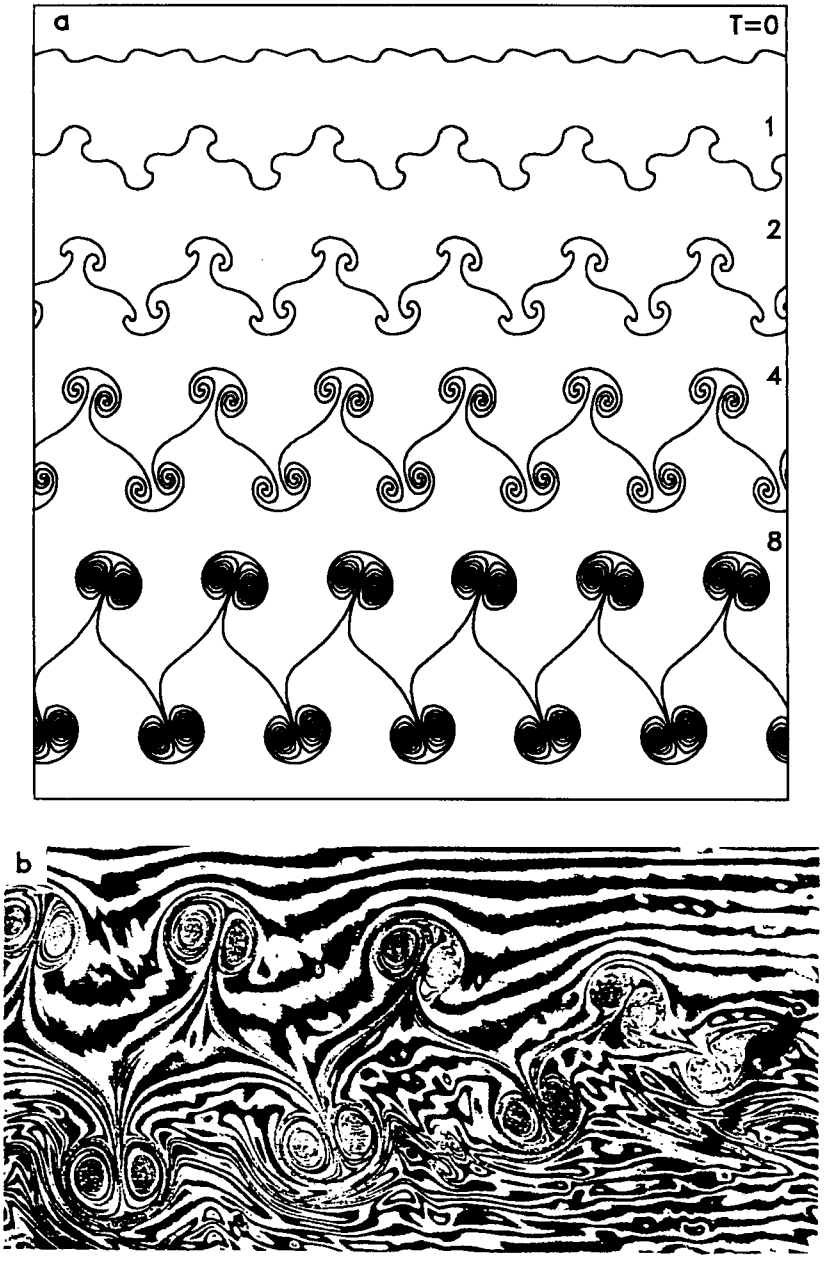

Figure 4.3 a) Computation using patched sinusoidal functions for the initial shape. b) Forcing at slightly different than the natural shedding frequency causes the vortex couples to propagate on both sides (experiment reproduced from Couder and Basdevant [14]).

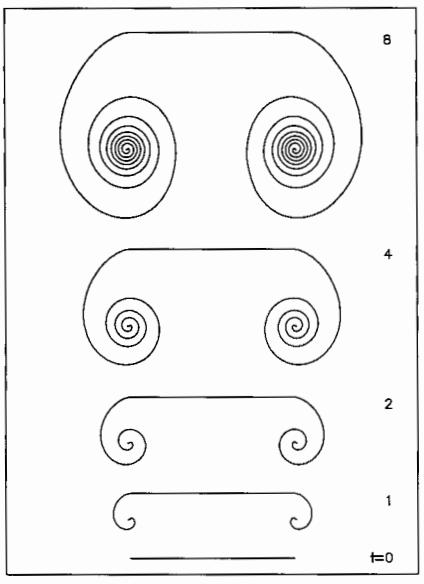

Figure 5.1 Desingularized vortex sheet roll-up due to the motion of a flat plate, computed using $\delta = 0.2$.

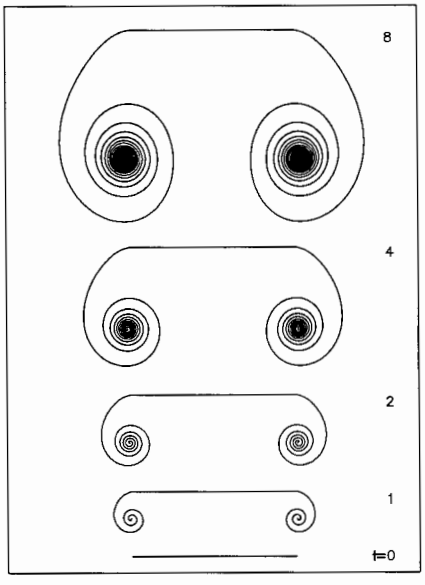

Figure 5.2 Desingularized vortex sheet roll-up due to the motion of a flat plate, computed using $\delta = 0.1$.

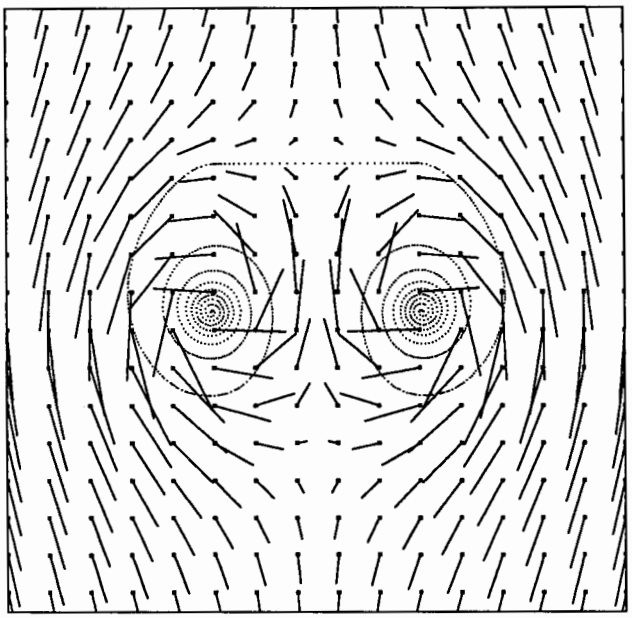

Figure 5.3 Velocity field for the $\delta = 0.2$ computation at time $t = 8$, in a frame of reference moving with the plate. The free vortex blobs and bound point vortices are plotted as a sequence of points.

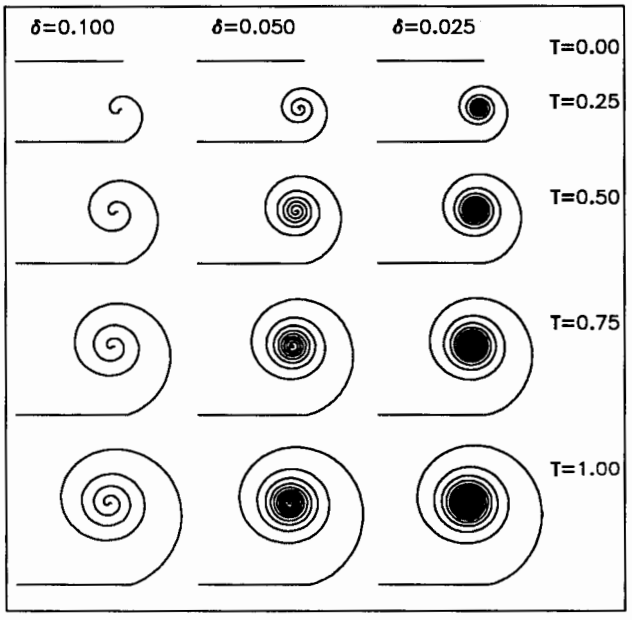

Figure 5.4 Self-similar vortex sheet roll-up past a semi-infinite flat plate. Computed solutions are presented for $0 \leq t \leq 1$ and $0.025 \leq \delta \leq 0.1$.

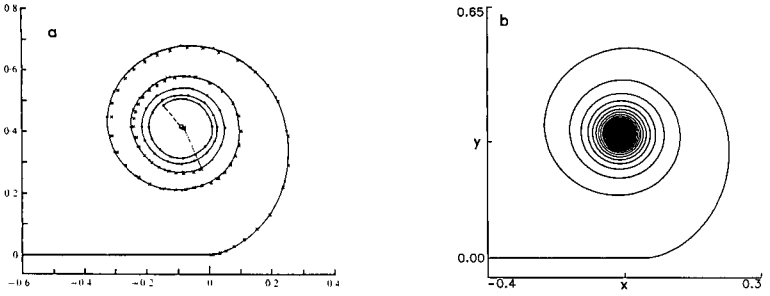

Figure 5.5 a) Pullin's computed result for self-similar roll-up (reproduced from [27]). b) Vortex blob result at $t = 1$ using $\delta = 0.025$. These plots may be superimposed to verify that they agree quite well.

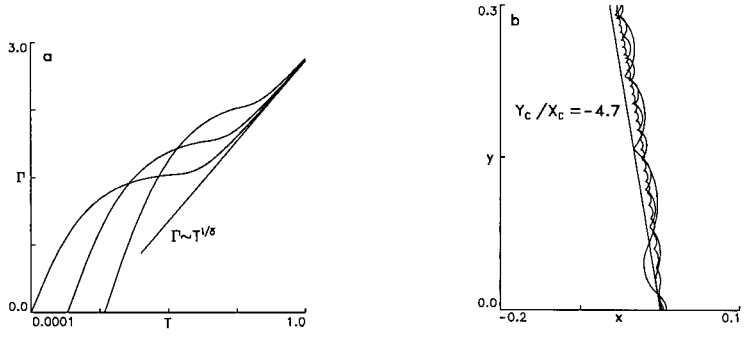

Figure 5.6 a) The total amount of shed circulation vs. time (log-log plot). b) The trajectory of the vortex core. The calculations used $\delta = 0.1, 0.05, 0.025$. The straight lines are self-similar scaling laws [27].

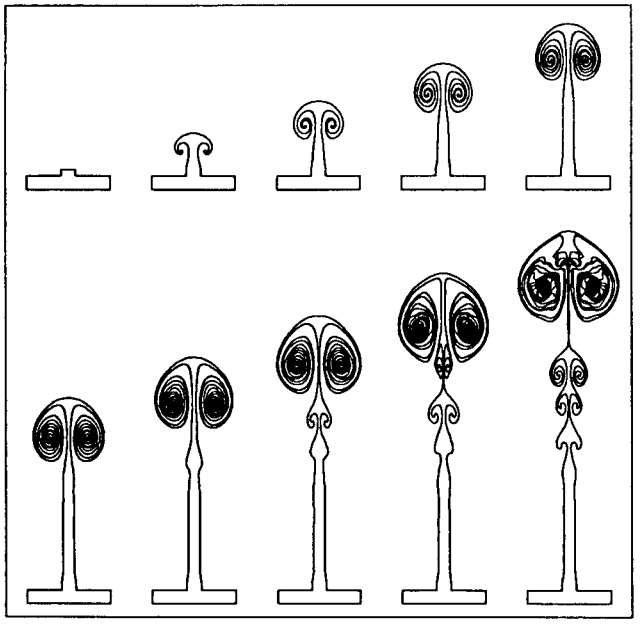

Figure 5.7 Computation of a jet being expelled from a box.

REFERENCES

1. F. H. Abernathy and R. E. Kronauer, *The Formation of Vortex Streets*, J. Fluid Mech. **13** (1962), 1-20.
2. C. Anderson and C. Greengard, *On Vortex Methods*, SIAM J. Numer. Anal. **22** (1985), 413-440.
3. H. Aref and E. Siggia, *Evolution and Breakdown of a Vortex Street in Two Dimensions*, J. Fluid Mech. **109** (1981), 435-463.
4. G. R. Baker and M. J. Shelley, *On the Connection Between Thin Vortex Layers and Vortex Sheets*, J. Fluid Mech. (1990 to appear).
5. G. Birkhoff, *Helmholtz and Taylor Instability, Proc. Symp. Appl. Math.*, Amer. Math. Soc., Providence, R. I., 1962, pp. 55-76.
6. D. R. Boldman, P. F. Brinich and M. E. Goldstein, *Vortex Shedding from a Blunt Trailing Edge with Equal and Unequal External Mean Velocities*, J. Fluid Mech. **75** (1976), 721-735.
7. C. Börgers, *On the Numerical Solution of the Regularized Birkhoff Equation*, Math. Comp. **53** (1989), 141-156.
8. R. Caflisch and O. Orellana, *Long Time Existence for a Slightly Perturbed Vortex Sheet*, Comm. Pure Appl. Math. **39** (1986), 807-838.
9. R. Caflisch and J. Lowengrub, *Convergence of the Vortex Method for Vortex Sheets*, SIAM J. Numer. Anal. **26** (1989), 1060-1080.
10. A. J. Chorin, *Numerical Study of Slightly Viscous Flow*, J. Fluid Mech. **57** (1973), 785-796.
11. A. J. Chorin and P. S. Bernard, *Discretization of a Vortex Sheet with an Example of Roll-up*, J. Comp. Phys. **13** (1973), 423-429.
12. M.-H. Chou, *A Numerical Method for Inviscid Two-Dimensional Flow Past an Inclined Plate*, PhD Thesis, Courant Institute of Mathematical Sciences (1985).
13. K. Chua, D. Lisoski, A. Leonard and A. Roshko, *A Numerical and Experimental Investigation of Separated Flow Past an Oscillating Flat Plate*, ASME Int. Symp. on Nonsteady Fluid Dynamics, eds. J. A. Miller and D. P. Telionis (1990 Toronto).
14. Y. Couder and C. Basdevant, *Experimental and Numerical Study of Vortex Couples in Two-Dimensional Flows*, J. Fluid Mech. **173** (1986), 225-251.
15. C. Basdevant, Y. Couder and R. Sadourny, *Vortices and Vortex Couples in Two Dimensional Turbulence or Long-Lived Couples are Batchelor's Couples*, Macroscopic Modelling of Turbulent Flows, Lecture Notes in Physics (Springer) **230** (1984), 327-346.
16. R. J. DiPerna and A. Majda Concentrations in Regularizations for 2-D Incompressible Flow, Comm. Pure Appl. Math. **XL** (1987), 301-345.
17. J. M. R. Graham, *Application of Discrete Vortex Methods to the Computation of Separated Flows*, Numerical Methods for Fluid Dynamics II edited by K. W. Morton and M. J. Baines, (1985), 273-302, Clarendon Press.
18. R. Krasny, *A Study of Singularity Formation in a Vortex Sheet by the Point Vortex Approximation*, J. Fluid Mech. **167** (1986), 65-93.
19. R. Krasny, *Desingularization of Periodic Vortex Sheet Roll-Up*, J. Comp. Phys. **65** (1986), 292-313.
20. R. Krasny, *Computation of Vortex Sheet Roll-up in the Trefftz Plane*, J. Fluid Mech. **184** (1987), 123-155.
21. R. Krasny, *A Vortex-Dipole Sheet Model for a Wake*, Phys. Fluids A **1** (1989), 173-175.
22. C. Lim and L. Sirovich, *Nonlinear Vortex Trail Dynamics*, Phys. Fluids **31** (1988), 991-998.
23. D. I. Meiron, G. R. Baker and S. A. Orszag, *Analytic Structure of Vortex Sheet Dynamics. 1. Kelvin-Helmholtz Instability*, J. Fluid Mech. **114** (1982), 283-298.
24. D. T. Mook and B. Dong, *Application of Vortex Dynamics to Simulations of Two Dimensional Wakes*, ASME Int. Symp. on Nonsteady Fluid Dynamics, eds. J. A. Miller and D. P. Telionis (1990 Toronto).
25. D. W. Moore, *The Spontaneous Appearance of a Singularity in the Shape of an Evolving Vortex Sheet*, Proc. Roy. Soc. Lond. A **365** (1979), 105-119.
26. C. Pozrikidis and J. J. L. Higdon, *Instability of Compound Vortex Layers and Wakes*, Phys. Fluids **30** (1987), 2965.

27. D. I. Pullin, *The Large-Scale Structure of Unsteady Self-Similar Rolled-up Vortex Sheets*, J. Fluid Mech. 88 (1978), 401-430.
28. N. Rott, *Diffraction of a Weak Shock with Vortex Generation*, J. Fluid Mech. 1 (1956), 111-128.
29. T. Sarpkaya, *An Inviscid Model of Two-Dimensional Vortex Shedding for Transient and Asymptotically Steady Separated Flow Over an Inclined Plate*, Journal of Fluid Mechanics 68 (1975), 109-128.
30. M. Shelley, *A Case of Singularity Formation in Vortex Sheet Motion Studied by a Spectrally Accurate Method*, preprint (1990).
31. C. Sulem, P. Sulem, C. Bardos and U. Frisch, *Finite Time Analyticity for the Two- and Three-Dimensional Kelvin-Helmholtz Instability*, Comm. Math. Phys. 80 (1981), 485-516.
32. S. Taneda and H. Honji, *Unsteady Flow past a Flat Plate Normal to the Direction of Motion*, Journal of the Physical Society of Japan 30 (1971), 262-272.
33. G. Tryggvason, *Simulations of Vortex Sheet Roll-Up by Vortex Methods*, J. Comput. Phys. 75 (1988), 253.
34. G. Tryggvason, W. J. A. Dahm and K. Sbeih, *Fine Structure of Vortex Sheet Roll-Up by Viscous and Inviscid Simulation*, ASME J. Fluids Engin., to appear (1990).

MATH DEPARTMENT, UNIVERSITY OF MICHIGAN, ANN ARBOR, MI 48109
E-MAIL ADDRESS: KRASNY@MATH.LSA.UMICH.EDU